PHYSICAL REVIEW E **88**, 010802(R) (2013)

Explosive synchronization in a general complex network

Xiyun Zhang,[1] Xin Hu,[1] J. Kurths,[2,3] and Zonghua Liu[1,2,*]

[1]*Department of Physics, East China Normal University, Shanghai, 200062, People's Republic of China*

[2]*Potsdam Institute for Climate Impact Research (PIK), DE-14473 Potsdam, Germany*

[3]*Institute of Physics, Humboldt University, DE-12489 Berlin, Germany*

(Received 24 January 2013; revised manuscript received 21 June 2013; published 15 July 2013)

Explosive synchronization (ES) has recently attracted much attention, where its two necessary conditions are found to be a scale-free network topology and a positive correlation between the natural frequencies of the oscillators and their degrees. Here we present a framework for ES to be observed in a general complex network, where a positive correlation between coupling strengths of the oscillators and the absolute of their natural frequencies is assumed and the previous studies are included as specific cases. In the framework, the previous two necessary conditions are replaced by another one, thus fundamentally deepening the understanding of the microscopic mechanism toward synchronization. A rigorous analytical treatment by a mean field is provided to explain the mechanism of ES in this alternate framework.

DOI: 10.1103/PhysRevE.88.010802 PACS number(s): 89.75.Hc, 89.75.Kd, 89.20.−a

Synchronization has recently been intensively investigated in complex networks [1]. It has been demonstrated that the network topology has a strong influence on the onset of synchronization, but it does not influence the feature of a continuous transition to synchronization, even in heterogeneous scale-free (SF) networks [2–7]. That is, this phase transition is always a second-order phase transition. However, this conclusion was recently challenged in SF networks of Kuramoto oscillators, where the phase transition was proved to be a first-order transition when the natural frequencies of the oscillators are positively correlated to the degrees of nodes [8].

This abrupt transition of a macroscopic state in a complex network is called *explosive synchronization* (ES) and has currently become a subject of utmost interest [8–13]. A crucial property of ES is the existence of a hysteresis at the transition to synchronization. ES was first revealed in a SF network of Kuramoto oscillators, provided that the natural frequency ω_i of each node i equals its degree k_i, i.e., $\omega_i = k_i$ [8]. Then it was extended to networks of chaotic units and confirmed by experiments of electronic circuits in a star configuration [9]. Very recently, it has been found that ES can have a new form of cluster explosive synchronization [12,13]. These works undoubtedly have opened a new window to critical phenomena. However, all these works are based on two necessary conditions: (1) The network is scale free, and (2) there is a positive correlation between the natural frequencies of the oscillators and their degrees. Here we challenge the necessity of these two conditions of ES and ask whether it is possible to observe ES in a non-SF network.

In this Rapid Communication, we present a framework to investigate ES in a general complex network by incorporating a positive correlation between coupling strengths of the oscillators and the absolute of their natural frequencies, where the previous studies are included as special cases. In this line, we show that ES may occur in both SF and non-SF networks for two classes of frequency distributions, i.e., (i) symmetric distributions with both positive and negative frequencies and (ii) asymmetric distributions with power-law frequency distributions. Through extensive numerical simulations, we will show that in our framework, ES can emerge in a general complex network such as a random, SF, and fully connected network, etc. Furthermore, a rigorous theoretical analysis is presented to explain its mechanism.

We consider a network of N coupled limit-cycle oscillators. Each oscillator is characterized by its phase $\theta_i(t)$, $i = 1, \ldots, N$, and obeys an equation of motion defined as [14]

$$\dot{\theta}_i = \omega_i + \frac{\lambda|\omega_i|}{\sum_{j=1}^{N} A_{ij}} \sum_{j=1}^{N} A_{ij} \sin(\theta_j - \theta_i), \quad i = 1, \ldots, N, \tag{1}$$

where λ is the overall coupling strength, ω_i is the natural frequency of oscillator i, and A_{ij} are the elements of the adjacency matrix A, so that $A_{ij} = 1$ when the nodes i and j are connected and $A_{ij} = 0$ otherwise. Equation (1) can be considered as a frequency-weighted network and reflects the feature of several natural and social systems. For example, a power grid network can be described as a network of Kuramoto oscillators, where the weighted coupling coefficient between two oscillators is related to their own natural frequencies [15,16]. In communication networks, an extrovert will contact his or her neighbors more frequently than an introvert. If we define the contact between two individuals as a kind of coupling and the frequency of contacts as coupling strength, the coupling strength will be correlated with the characteristics of individuals, i.e., a kind of natural frequency of human being [16].

There are two characteristic features in Eq. (1): One is the positive correlation between coupling strengths of the oscillators and the absolute of their natural frequencies. Another is the average part $\frac{1}{\sum_{j=1}^{N} A_{ij}} \sum_{j=1}^{N} A_{ij} \sin(\theta_j - \theta_i)$, which makes the contribution from the $k_i \equiv \sum_{j=1}^{N} A_{ij}$ neighbors be equivalent to one average coupling. In this sense, we may regard each node as having only one link with the average coupling, which significantly reduces the effect of heterogeneity of network topology in ES. As the general Kuramoto model, we let the frequencies ω_i satisfy a distribution $g(\omega)$. We focus on

*zhliu@phy.ecnu.edu.cn

two classes of $g(\omega)$: (i) symmetric $g(\omega)$ such as the random, Lorentzian, or Gaussian distributions, and (ii) asymmetric $g(\omega)$ such as power-law frequency distributions.

Class I—symmetric $g(\omega)$. In this case, Eq. (1) is substantially different from the original scenario of ES discussed in Refs. [8–11] in three aspects: (i) ω_i can be both positive and negative in Eq. (1) but only positive in [8–11]; (ii) the network topology can be both SF and non-SF in Eq. (1) but only SF in Refs. [8–11]; and (iii) ω_i is independent of k_i in Eq. (1) but with $\omega_i = k_i$ in [8–11]. Excepting these differences, we notice that the absolute of ω_i in Eq. (1) is also important, which will be explained later by both numerical simulations and theoretical analysis.

In numerical simulations, we take into account networks generated by (i) fully connected networks, (ii) random Erdős-Rényi (ER) networks, and (iii) SF networks of the uncorrelated configuration model (UCM) with a power-law degree distribution [17]. We let the size of all the networks be $N = 500$ in this Rapid Communication. To measure the coherence of the collective motion, we use the order parameter R [7,8],

$$Re^{i\Psi} = \frac{1}{N}\sum_{j=1}^{N} e^{i\theta_j}, \tag{2}$$

where Ψ denotes the average phase, and R $(0 \leqslant R \leqslant 1)$ is a measure of phase coherence. R will reach unity when the system is fully synchronized and be 0 for an incoherent solution. We increase the coupling strength λ adiabatically with an increment $\delta\lambda = 0.02$ from $\lambda = 0$ and compute the stationary value of the order parameter R for each λ.

In the case of a fully connected network, here we consider two typical distributions of the natural frequencies $g(\omega)$, i.e., Lorentzian and Gaussian distributions, but the obtained results also work for other symmetric distributions such as random distributions. The Lorentzian distribution has the expression $g(\omega) = \frac{1}{\pi}[\frac{\gamma}{(\omega-\omega_0)^2+\gamma^2}]$ with the central frequency ω_0 and γ is the half width at half maximum [18]. The Gaussian distribution follows $g(\omega) = \frac{1}{\sqrt{2\pi}\sigma}\exp(-\frac{(\omega-\mu)^2}{2\sigma^2})$ with the mean μ and variance σ^2. Without loss of generality, we take $\omega_0 = 0$, $\gamma = 0.5$, $\mu = 0$, and $\sigma^2 = 1$ in this Rapid Communication. Figures 1(a) and 1(b) show the dependence of R on λ for the Lorentzian and Gaussian distributions, respectively, where the squares and circles represent the cases of forward and backward continuations in λ, respectively. In the cases of ER and UCM networks, we take the Lorentzian distribution of the natural frequencies $g(\omega)$ and let the average degree be $\langle k\rangle = 6$. Figures 1(c) and 1(d) show the results. We find that there are two sharp transitions in each panel of Fig. 1 at a λ_{cF} from the forward continuation diagram and λ_{cB} from the backward continuation diagram, which form a hysteresis and thus indicate that a first-order synchronization transition appears in both SF and non-SF networks.

To deeply analyze the change of the order of synchronization transition, we follow Ref. [8] and compute the effective frequency along the forward continuation as $\omega_i^{\text{eff}} = \frac{1}{T}\int_t^{t+T}\dot{\theta}_i(\tau)d\tau$ with $T \gg 1$. We take the case of Fig. 1(a) as an example and focus on the forward continuation in λ. Figure 2(a) shows the result. From Fig. 2(a) we observe that

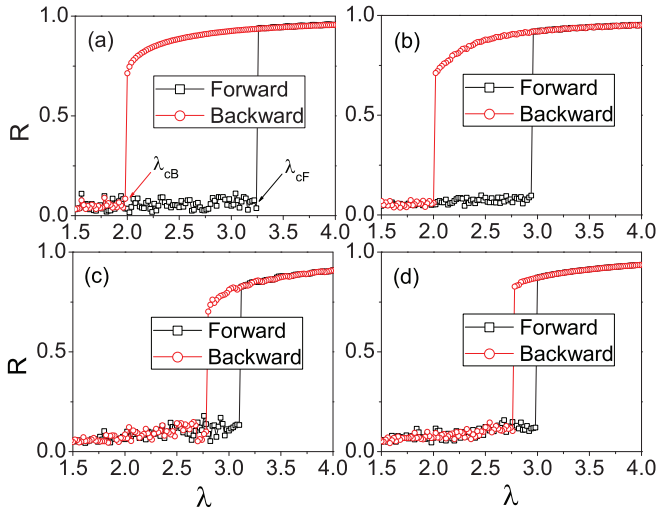

FIG. 1. (Color online) Synchronization diagrams for different networks. (a) and (b) represent the cases of a fully connected network for the Lorentzian and Gaussian distributions, respectively, with $\omega_0 = 0$ and $\gamma = 0.5$ in (a) and $\mu = 0$ and $\sigma^2 = 1$ in (b). (c) and (d) represent the cases of ER and UCM networks, respectively, with the Lorentzian distribution of the natural frequencies and average degree $\langle k\rangle = 6$.

all the ω_i^{eff} will retain their natural frequencies before the synchronization transition and then they suddenly jump to the average frequency of $\langle\omega\rangle = \frac{1}{N}\sum_{j=1}^{N}\omega_i$ at the critical point λ_{cF}, which signals the onset of ES observed in Fig. 1(a).

To further explore the evolution of the phases, in Fig. 2(b) we show the dependence of $\Delta\theta_i$ on the forward continuation in λ with $\Delta\theta_i = \theta_i - \Psi$. Interestingly, we find that $\Delta\theta_i$ do not jump to zero at the critical point λ_{cF}, but suddenly concentrate on two different values, indicating that the oscillators have been divided into two synchronization clusters. We will explain this point in the theoretical part.

To study the role of taking the absolute of ω_i in Eq. (1), we replace $|\omega_i|$ by ω_i. In this situation, our numerical

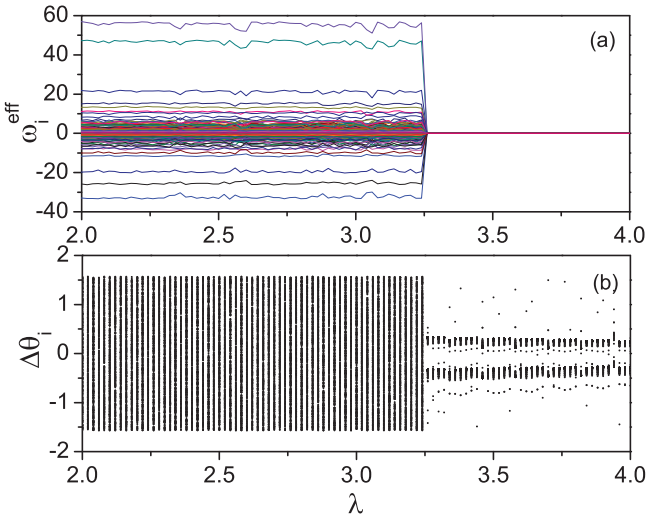

FIG. 2. (Color online) The evolutionary dynamics along the forward continuation in the network model of Fig. 1(a). (a) ω_i^{eff} vs λ. (b) $\Delta\theta_i$ vs λ.

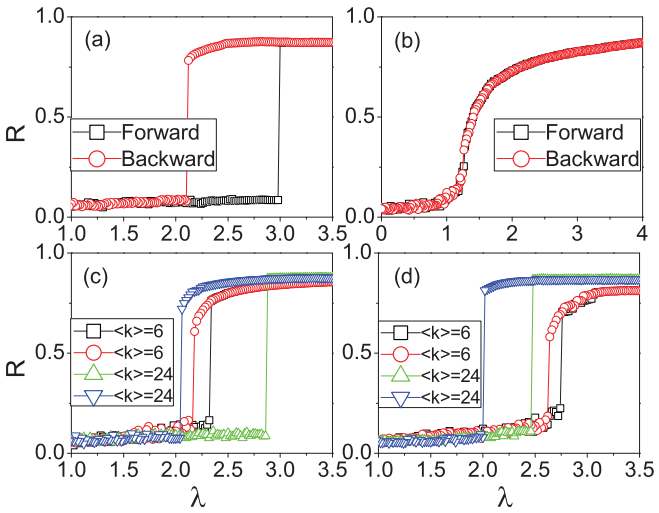

FIG. 3. (Color online) Case of class II. The curves with squares and circles in (a)–(d) correspond to Figs. 1(a)–1(d), respectively, where $g(\omega) \sim \omega^{-\beta}$ with $\omega > 0$ and $\beta = 1.5$ in (a), (c), and (d), and $g(\omega) = \sqrt{\frac{2}{\pi}} \exp(-\frac{\omega^2}{2})$ with $\omega > 0$ in (b). The curves with up triangles and down triangles in (c) and (d) denote the case of $\langle k \rangle = 24$.

simulations show that ES cannot be observed in all the cases of Figs. 1(a)–1(d), indicating that the absolute of ω_i is the key to induce ES in the framework of Eq. (1).

Class II—asymmetric $g(\omega)$. In this case, we replace the Lorentzian distribution by a power-law distribution $g(\omega) \sim \omega^{-\beta}$ with $\omega > 0$. Specifically, the original scenario of ES in Refs. [8–11] can be expressed as a particular case of class II when the network is SF and $\omega_i = k_i$. We also replace the Gaussian distribution in Fig. 1(b) by $g(\omega) = \sqrt{\frac{2}{\pi}} \exp(-\frac{\omega^2}{2})$ with $\omega > 0$. The curves with squares and circles in the four panels of Fig. 3 show the results corresponding to the cases of Figs. 1(a)–1(d), respectively. We see that there is a hysteresis in Figs. 3(a), 3(c), and 3(d) but no hysteresis in Fig. 3(b). We will explain this point in the theoretical part. We also notice that the loop size of the hysteresis in Figs. 3(c) and 3(d) is much smaller than that in Fig. 3(a). This difference may come from the fact that the average degree in Fig. 3(a) is much larger than that in Figs. 3(c) and 3(d). To confirm it, we increase the average degree in Figs. 3(c) and 3(d) from $\langle k \rangle = 6$ to $\langle k \rangle = 24$. The curves with up triangles and down triangles in Figs. 3(c) and 3(d) show the results. We see that the loop size of hysteresis for $\langle k \rangle = 24$ is much larger than that for $\langle k \rangle = 6$, thus confirming our analysis.

Analytical explanations for class I. We first consider the case of a fully connected network. From Eq. (2) we have $R \sin(\Psi - \theta_i) = \frac{1}{N} \sum_j \sin(\theta_j - \theta_i)$. Substituting it into Eq. (1), we obtain

$$\dot{\theta}_i = \omega_i + \lambda |\omega_i| R \sin(\Psi - \theta_i), \quad i = 1, \ldots, N. \tag{3}$$

We set a reference frame rotating with the average phase of the system, $\Psi(t) = \Psi(0) + \langle \omega \rangle t$, where $\langle \omega \rangle$ is the average frequency of the oscillators. For a symmetric distribution of $g(\omega)$, we have $\langle \omega \rangle = 0$. Letting $\Delta\theta_i \equiv \theta_i - \Psi$, then Eq. (1) becomes

$$\Delta\dot{\theta}_i = \omega_i - \lambda |\omega_i| R \sin(\Delta\theta_i), \quad i = 1, \ldots, N. \tag{4}$$

When all the oscillators are phase locked, we have $\Delta\dot{\theta}_i = 0$ and thus get

$$\Delta\theta_i = \begin{cases} \arcsin\left(\frac{1}{\lambda R}\right), & \omega_i > 0, \\ \arcsin\left(-\frac{1}{\lambda R}\right), & \omega_i < 0. \end{cases} \tag{5}$$

Equation (5) implies that in the phase-locked status, the oscillators will split into two equal clusters with half in the state of $\Delta\theta_i = \arcsin\left(\frac{1}{\lambda R}\right)$ and the other half in the state of $\Delta\theta_i = \arcsin\left(-\frac{1}{\lambda R}\right)$, and both of them will gradually approach to zero with increasing λ. This result has been confirmed by Fig. 2(b). As $\Delta\theta_i$ does not depend on its value of ω_i, all the oscillators are in the same position of a synchronized state, i.e., a feature of ES. In this case, from Eq. (2) we get

$$R = \frac{1}{N} \sum_{j=1}^{N} e^{i\Delta\theta_j} = \frac{1}{2}(e^{i\Delta\theta_+} + e^{i\Delta\theta_-}), \tag{6}$$

where $\Delta\theta_+$ and $\Delta\theta_-$ represent the two groups in Eq. (5). Substituting Eq. (5) into Eq. (6), we obtain $R = \frac{1}{2}(\cos\Delta\theta_+ + \cos\Delta\theta_-)$, which gives

$$R^2 = \frac{\lambda + \sqrt{\lambda^2 - 4}}{2\lambda}. \tag{7}$$

This result does not depend on the specific distribution of $g(\omega)$, provided it is symmetric. Equation (7) implies that ES exists only for $\lambda \geqslant 2$ and satisfies $R > \sqrt{0.5} \approx 0.707$. The critical point $\lambda_c = 2$ has been confirmed in Figs. 1(a) and 1(b) by $\lambda_{cB} = 2$. Considering $R \approx 0$ for an unsynchronized status, R will have a big jump from 0.707 to 0 at the synchronization transition, indicating a first-order phase transition.

To show the important role of the absolute of ω_i for ES to appear in Eq. (1), we consider its corresponding case without the absolute. In this situation, the two equations in Eq. (5) will become one $\Delta\theta_+ = \arcsin\left(\frac{1}{\lambda R}\right)$ for both $\omega_i > 0$ and $\omega_i < 0$. Substituting it into Eq. (6) we yield

$$R = \frac{1}{N} \sum_{j=1}^{N} e^{i\Delta\theta_j} = e^{i\Delta\theta_+} = \cos(\Delta\theta_+) + i \sin(\Delta\theta_+). \tag{8}$$

To guarantee a real R, the imaginary part $\sin(\Delta\theta_+)$ in Eq. (8) has to be zero, which requires $\lambda \to \infty$. That is, we will not observe ES for a finite λ. This explains our findings in the numerical simulations.

We now turn to the case of non-fully-connected networks, such as ER and UCM. For an uncorrelated network, we follow Refs. [7,10] to rewrite Eq. (1) as

$$\dot{\theta}(t) = \omega + \lambda |\omega| \int dk' \int d\theta' \frac{k' P(k')}{\langle k \rangle} \rho(k'; \theta', t) \sin(\theta' - \theta) - \lambda |\omega| h(t), \tag{9}$$

where $P(k), \langle k \rangle, \rho(k; \theta, t)$ represent the degree distribution, average degree, and density of the nodes with phase θ at time t for a given degree k, respectively, and the term $h(t)$ takes into account time fluctuations and is given by $h = \mathrm{Im}\{e^{-i\theta} \sum_{j=1}^{N} A_{ij} (\langle e^{i\theta_j} \rangle_t - e^{i\theta_j})\}$, where Im stands for the imaginary part. For the thermodynamic limit, the term $h(t)$ can be neglected when the average degree $\langle k \rangle$ is

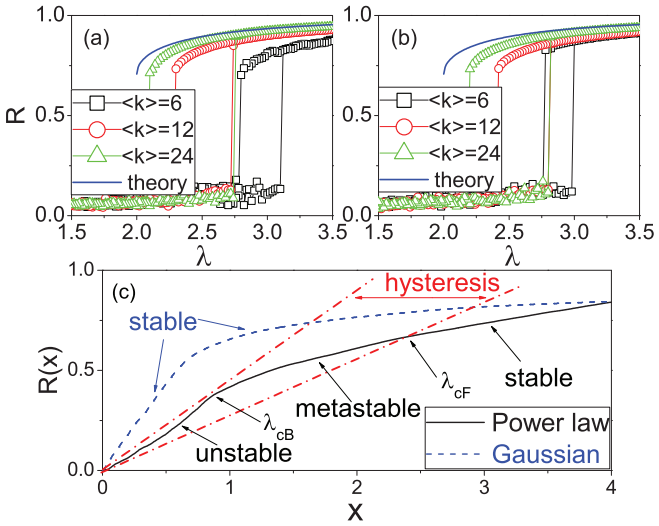

FIG. 4. (Color online) (a) and (b) represent the cases of ER and UCM networks in class I, respectively, where the curves with squares, circles, and triangles represent the cases of $\langle k\rangle = 6$, 12, and 24, respectively, and the solid curve represents the theoretical result from Eq. (7). (c) $R(x)$ vs x for fully connected networks in class II where the solid and dashed curves correspond to Figs. 3(a) and 3(b), respectively.

large enough [7]. Correspondingly, Eq. (2) can be rewritten as

$$Re^{i\Psi} = \frac{1}{\langle k\rangle}\int dk \int d\theta k P(k)\rho(k;\theta,t)e^{i\theta}, \tag{10}$$

which gives $R\sin(\Psi-\theta) = \frac{1}{\langle k\rangle}\int dk \int d\theta' k P(k)\rho(k;\theta',t)\sin(\theta'-\theta)$. Neglecting the fluctuation $h(t)$ and substituting Eq. (10) into Eq. (9), we obtain

$$\dot{\theta}(t) = \omega + \lambda|\omega| R\sin(\Psi-\theta). \tag{11}$$

This is exactly Eq. (3). Therefore, the results obtained from Eq. (3) should also work for the case of non-fully-connected networks, provided that the term $h(t)$ in Eq. (9) can be neglected. In numerical simulations, networks with a larger average degree $\langle k\rangle$ will better satisfy the mean-field approximation (9)–(11). Figures 4(a) and 4(b) show the dependence of R on different average degrees $\langle k\rangle$ for ER and UCM networks, respectively, where the curves with squares, circles, and triangles represent the cases of $\langle k\rangle = 6$, 12, and 24, respectively, and the solid curve represents the theoretical result from Eq. (7). We find that with increasing $\langle k\rangle$, the backward R curves move towards the theoretical curve, confirming our theoretical analysis.

Analytical explanations for class II with $\omega_i > 0$. We first consider the case of a fully connected network. By doing the same derivation as Eq. (4) we obtain

$$\Delta\dot{\theta}_i = \omega_i - \langle\omega\rangle - \lambda\omega_i R\sin(\Delta\theta_i). \tag{12}$$

Then, doing the same derivation steps of Refs. [10,11], we get

$$R(x) = \int \sqrt{1-\left(\frac{\omega-\langle\omega\rangle}{x\omega}\right)^2}\, g(\omega)\Theta\left(1-\left|\frac{\omega-\langle\omega\rangle}{x\omega}\right|\right)d\omega, \tag{13}$$

where $x = R\lambda$ and $\Theta(x)$ is the Heaviside step function. Figure 4(c) shows the solution of Eq. (13) where the solid and dashed curves correspond to the cases of Figs. 3(a) and 3(b), respectively. Figure 4(c) can be well explained by following Ref. [11]. We first consider the case of the solid curve, i.e., the case of power-law distribution. For this case, the red dashed-dotted line has a slope of $1/\lambda$ and its intersection with $R(x)$ will give the order parameter R. For a given λ, there will be only one intersection (i.e., the origin) when $\lambda < \lambda_{cB}$ but three intersections when $\lambda_{cB} < \lambda < \lambda_{cF}$. Once λ is decreased to pass λ_{cB}, R will jump from the metastable state to zero, indicating a first-order transition. As the part of $R(x)$ between the origin and the point λ_{cB} is unstable, the stable origin and the metastable state constitute the region of the hysteresis. Then, we discuss the case of the blue dashed curve in Fig. 4(c). In this case, there is no part of three intersections, indicating no hysteresis there. Thus, Figs. 3(a) and 3(b) can be understood from Fig. 4(c). For the cases of non-fully-connected networks in Figs. 3(c) and 3(d), we can follow the steps from Eqs. (9) to (11) to obtain $\Delta\dot{\theta}_i = \omega_i - \langle\omega\rangle - \lambda\omega_i R\sin(\Delta\theta_i)$ when the fluctuation is neglected, which is exactly Eq. (12). Therefore, the ES in Figs. 3(c) and 3(d) can be also understood from Fig. 4(c).

In conclusion, we have presented a framework for ES to be observed in a general complex network and have given a rigorous analytical treatment. We find that both the effective coupling strength $\lambda|\omega_i|R$ in Eq. (4) for class I and $\lambda\omega_i R$ in Eq. (12) for class II show a common feature, i.e., a positive correlation between the effective coupling strength in the mean-field framework and the natural frequencies of the oscillators, which implies that both the ES of previous studies on network topology and the ES of Eq. (1) on coupling strength can be unified in the mean-field framework, and thus the previous two necessary conditions of ES can be replaced by the common feature.

We thank the anonymous referees for helpful comments. This work was partially supported by the NNSF of China under Grant No. 11135001, 973 Program under Grant No. 2013CB834100, and by IRTG/GRK 1740.

[1] A. Arenas, A. Diaz-Guilera, J. Kurths, Y. Moreno, and C. Zhou, Phys. Rep. **469**, 93 (2008).

[2] A. Arenas, A. Diaz-Guilera, and C. J. Perez-Vicente, Phys. Rev. Lett. **96**, 114102 (2006).

[3] J. Gomez-Gardenes, Y. Moreno, and A. Arenas, Phys. Rev. Lett. **98**, 034101 (2007).

[4] M. Barahona and L. M. Pecora, Phys. Rev. Lett. **89**, 054101 (2002).

[5] T. Nishikawa, A. E. Motter, Y. C. Lai, and F. C. Hoppensteadt, Phys. Rev. Lett. **91**, 014101 (2003).

[6] T. Ichinomiya, Phys. Rev. E **70**, 026116 (2004).

[7] J. G. Restrepo, E. Ott, and B. R. Hunt, Phys. Rev. E **71**, 036151 (2005).

[8] J. Gómez-Gardeñes, S. Gómez, A. Arenas, and Y. Moreno, Phys. Rev. Lett. **106**, 128701 (2011).

[9] I. Leyva, R. Sevilla-Escoboza, J. M. Buldu, I. Sendina-Nadal, J. Gomez-Gardenes, A. Arenas, Y. Moreno, S. Gomez, R. Jaimes-Reategui, and S. Boccaletti, Phys. Rev. Lett. **108**, 168702 (2012).

[10] T. K. D. M. Peron and F. A. Rodrigues, Phys. Rev. E **86**, 056108 (2012); **86**, 016102 (2012).

[11] B. C. Coutinho, A. V. Goltsev, S. N. Dorogovtsev, and J. F. F. Mendes, Phys. Rev. E **87**, 032106 (2013).

[12] W. Liu, Y. Wu, J. Xiao, and M. Zhan, Europhys. Lett. **101**, 38002 (2013).

[13] P. Ji, T. K. DM. Peron, P. J. Menck, F. A. Rodrigues, and J. Kurths, Phys. Rev. Lett. **110**, 218701 (2013).

[14] Our numerical simulations show that ES can be still observed in Eq. (1) when $|\omega_i|$ is replaced by $|\omega_i|^\alpha$ with $\alpha \in (0,2)$.

[15] F. Dorfler and F. Bullo, in *Proceedings of the American Control Conference* (IEEE, Baltimore, 2010), p. 930.

[16] H. Wang and X. Li, Phys. Rev. E **83**, 066214 (2011).

[17] M. Catanzaro, M. Boguna, and R. Pastor-Satorras, Phys. Rev. E **71**, 027103 (2005).

[18] P. C. Matthews, R. E. Mirollo, and S. H. Strogatz, Physica D **52**, 293 (1991).